NUSC Technical Document 6551
29 September 1981

(12) LEVEL II

AD A105590

ANZUS Eddy II: Further Acoustic Modeling of an East Australian Current Eddy

A Paper Presented at the Tenth International Congress on Acoustics, 9-16 July 1980, Sydney, Australia

P. D. Scully-Power
Office of the Associate
Technical Director for Technology

D. G. Browning
Surface Ship Sonar Department

Naval Underwater Systems Center
Newport, Rhode Island / New London, Connecticut

Preface

This document was prepared under the sponsorship of the Naval Material Command under NUSC Project No. A65410, "Acoustic Variability Within the Sound Channel," as part of the NUSC Independent Research Program; NAVMAT Program Manager, CAPT D. F. Parrish, and NUSC Principal Investigator, D. G. Browning.

Reviewed and Approved: 29 September 1981

W. A. Von Winkle

W. A. Von Winkle
Associate Technical Director
for Technology

The authors of this document are located at the
New London Laboratory, Naval Underwater Systems Center,
New London, Connecticut 06320.

NUSC - REPORT DOCUMENTATION PAGE

READ INSTRUCTIONS BEFORE COMPLETING FORM

1. REPORT NUMBER TD-6551	2. GOVT ACCESSION NO. AD-A105590
3. RECIPIENT'S CATALOG NUMBER	
4. TITLE (and Subtitle) ANZUS Eddy II: Further Acoustic Modeling of an East Australian Current Eddy, A Paper Presented at the Tenth International Congress on Acoustics, 9-16 July 1980, Sydney, Australia	5. TYPE OF REPORT & PERIOD COVERED
	6. PERFORMING ORG. REPORT NUMBER
7. AUTHOR(s) P. D. Scully-Power and D. G. Browning	8. CONTRACT OR GRANT NUMBER(s)
9. PERFORMING ORGANIZATION NAME AND ADDRESS Naval Underwater Systems Center New London Laboratory New London, CT 06320	10. PROGRAM ELEMENT, PROJECT, TASK AREA & WORK UNIT NUMBERS A65410
11. CONTROLLING OFFICE NAME AND ADDRESS Naval Material Command Washington, DC 20360	12. REPORT DATE 29 Sep[illegible]81 13. NUMBER OF PAGES 14
14. MONITORING AGENCY NAME & ADDRESS (if different from Controlling Office)	15. SECURITY CLASS. (of this report) UNCLASSIFIED 15a. DECLASSIFICATION / DOWNGRADING SCHEDULE

16. DISTRIBUTION STATEMENT (of this Report)

Approved for public release; distribution unlimited.

17. DISTRIBUTION STATEMENT (of the abstract entered in Block 20, if different from Report)

18. SUPPLEMENTARY NOTES

19. KEY WORDS (Continue on reverse side if necessary and identify by block number)

East Australian Current
Ocean Eddies
Ocean Inhomogeneities
Warm Core Eddies

20. ABSTRACT (Continue on reverse side if necessary and identify by block number)

This document presents the oral and visual presentation entitled "ANZUS Eddy II: Further Acoustic Modeling of an East Australian Current Eddy," presented at the Tenth International Congress on Acoustics, 9-16 July 1980 in Sydney, Australia.

The dynamics of the South Coral and Tasman Seas has recently been shown to be governed by the East Australian Current and the Tasman Front; the current flowing south along the coast of Australia and then turning east around

DD FORM 1 JAN 73 1473

405918

20. (Continued)

34°S to feed the front that has the form of a planetary wave with a zonal wavevector. This planetary wave spawns warm core eddies to the south and cold core eddies to the north in a regular manner, conforming to theoretical postulates that such systems are controlled by a conservation of potential vorticity in which the linear and nonlinear effects are approximately of equal magnitude. These features, which cause a perturbation to the ocean's regular sound speed structure, can be scaled in a canonical manner, allowing a deterministic evaluation of their effects on an acoustic wave propagating through them. These effects have been calculated in the frequency band 30 Hz to 3 kHz using range dependent propagation models and show significant departures from an unperturbed ocean; the results have a direct application in the inverse problem of acoustic tomography.

ANZUS EDDY II: Further Acoustic Modeling of an East Australian Current Eddy

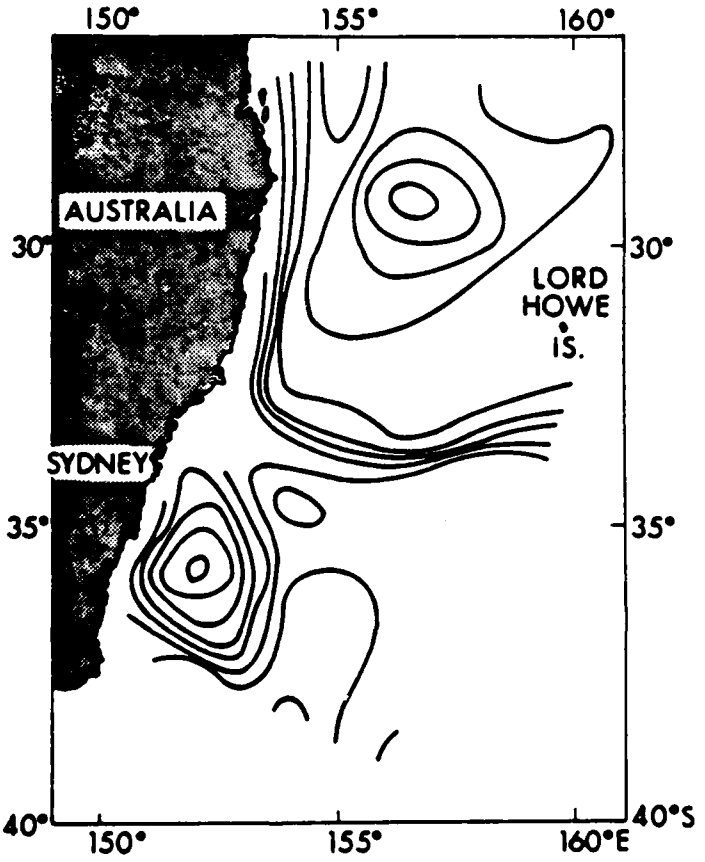

Slide 1

Ocean eddies — large rotating masses of water usually spun off from major currents — have only recently attracted the attention of both oceanographers and underwater acousticians.

One of the principal sites of scientific investigation is located nearby — just off the coast of eastern Australia where the East Australian current generates several large warm core eddies a year. Some of these eddies apparently remain at approximately the same location for an extended period of time.

This paper will review our work to determine the effect of these eddies on the transmission of sound in the sea and describe our latest acoustic modeling results.

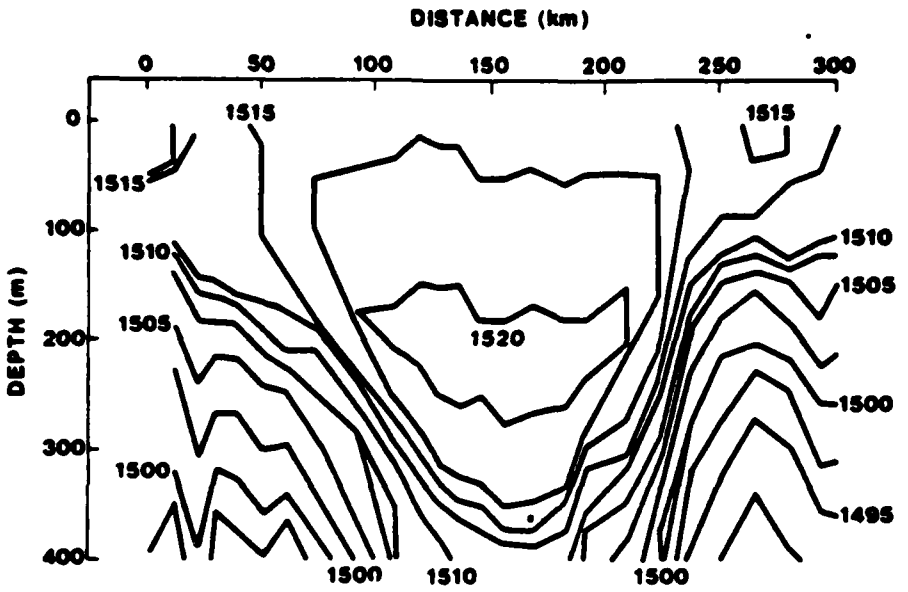

SOUND VELOCITY CROSS SECTION

Slide 2

A cross section of sound speed contours shows the extent of a typical warm core ocean eddy. The width about 250 kilometers, the depth at least 400 meters. A sound source located at a depth of, say, 300 meters would be at a significantly different sound speed inside the eddy than it would outside. This of course implies that sound would be refracted differently in each case.

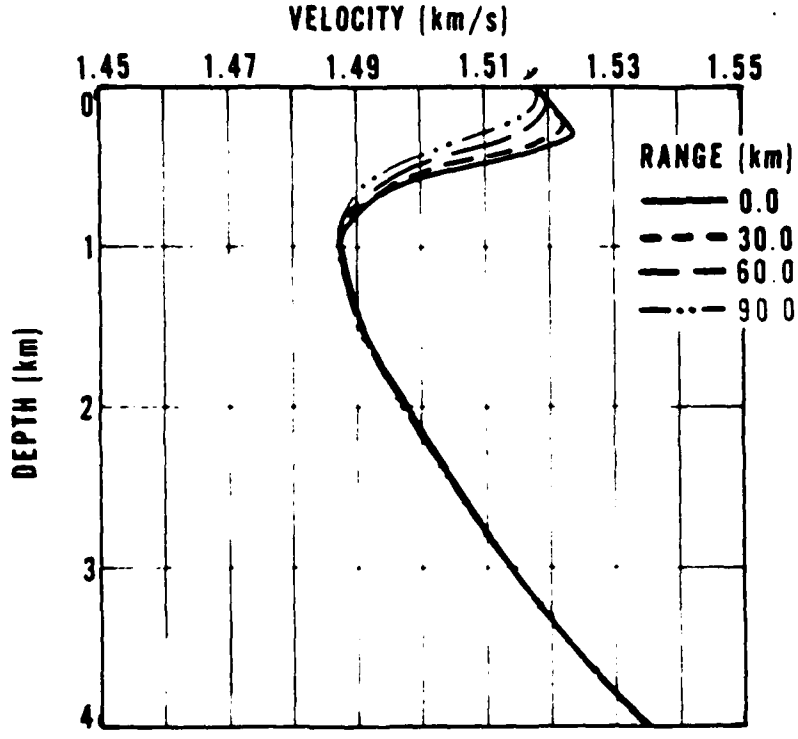

MODEL EDDY VELOCITY PROFILES
HALF-SECTION CENTER TO EDGE

Slide 3

In order to estimate the effect of an eddy on sound propagation, we first employed a range dependent, ray-theory, sound propagation prediction model developed by H. Weinberg of NUSC. The four sound speed profiles used were obtained from oceanographic data taken in an East Australian eddy. The results I will describe will be for sound propagation from the center to the edge of the eddy; hence, the sound speed profile for the center of the eddy is shown as range 0 kilometers, with outer edge profile at 90 kilometers.

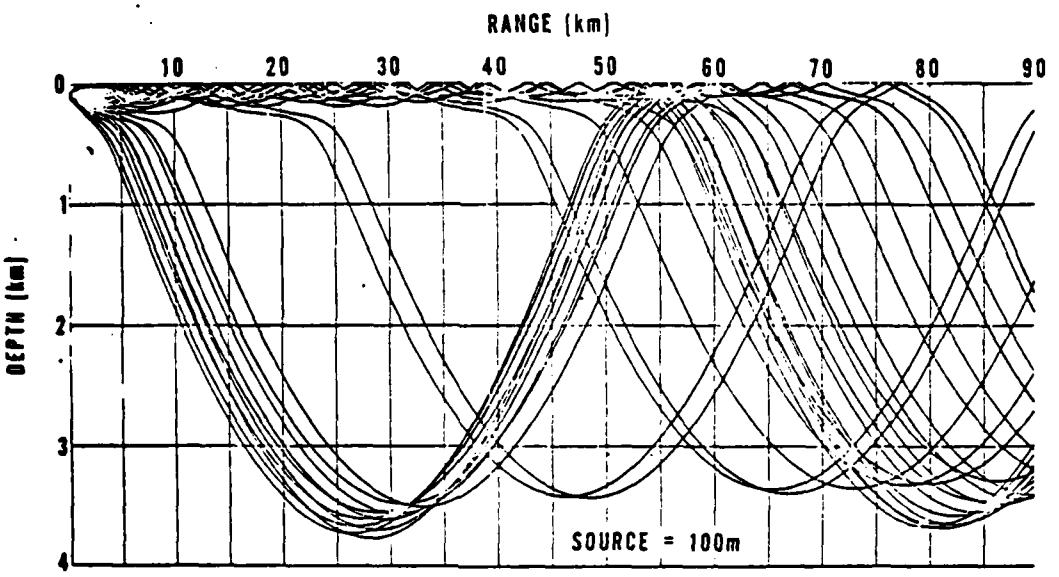

MODEL EDDY CENTER TO EDGE

Slide 4

A ray diagram illustrates the effect of the eddy. Without the eddy, the deep ocean sound speed profile would cause sound rays from a shallow source (say, 100 meters) to be refracted to a deep depth, returning at a range of approximately 60 kilometers to form a convergence zone.

With the eddy, the convergence zone still exists although more diffuse. However, for a shallow receiver energy is now channeled by an eddy duct so that there is no shadow zone between 10 and 50 kilometers. This ducting gradually tapers off as the channel narrows.

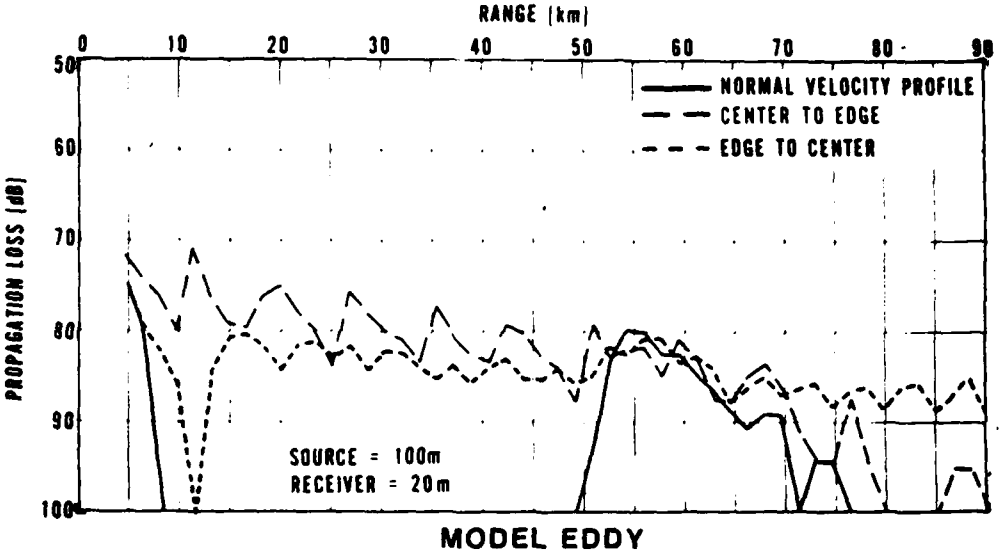

Slide 5

The predicted propagation loss follows the ray diagram. For a shallow source and receiver (100 meters and 20 meters, respectively), the non-eddy (normal) case has a rapid drop off to a shadow zone, followed by an increase of level at the convergence zone.

Propagating from the center of the eddy, there is only a gradual decline to the convergence zone then a blending to the non-eddy case as the edge is reached.

Propagating from the edge of the eddy, similar behavior is noted, except that the level remains relatively high beyond the convergence zone, i.e., near the center of the eddy.

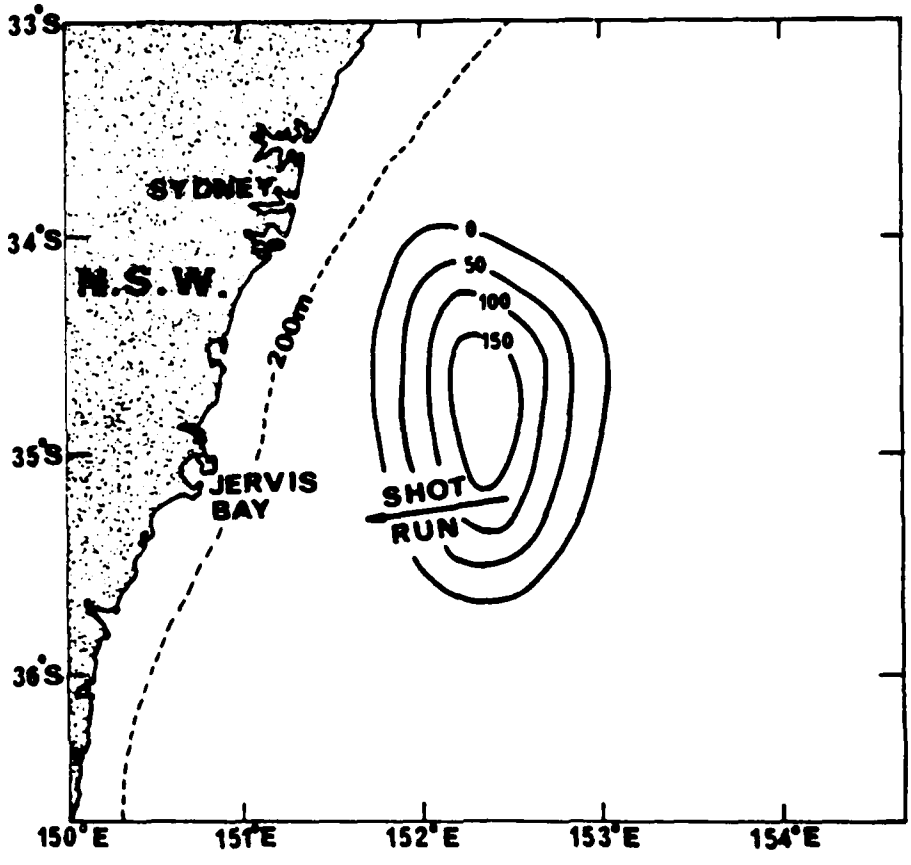

SHOT RUN AND EDDY LAYER THICKNESS (m)
20 MAR. 1975

Slide 6

In order to verify these predictions, a joint Australian, New Zealand, United States measurement program — called Project ANZUS Eddy — was conducted in an East Australian Current Eddy. A hydrophone was located near the center of the eddy and sound was transmitted to it at various ranges out to the edge of the eddy.

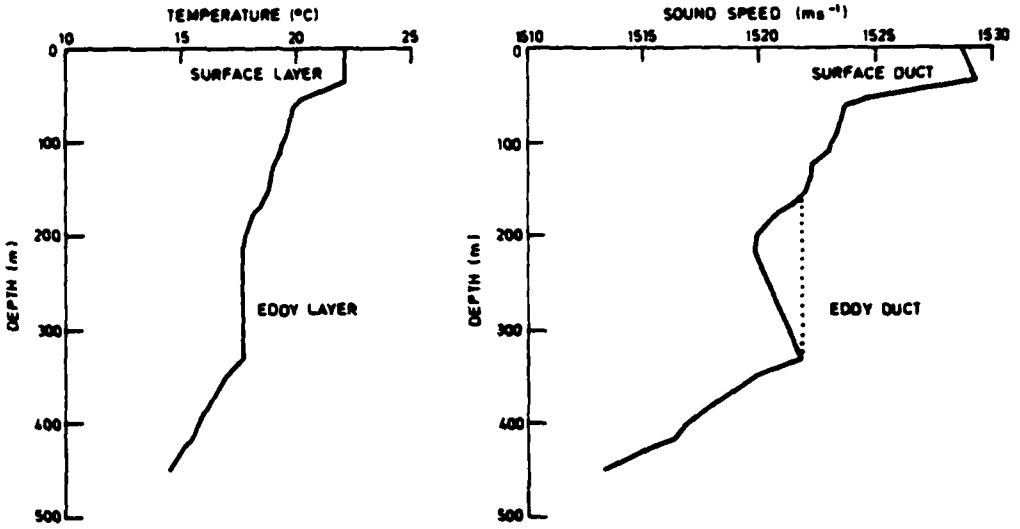

TEMPERATURE AND SOUND SPEED PROFILES AT RECEIVER, 20 MAR. 1975.

Slide 7

This experiment was conducted in the summer and it was found that a shallow, warm, mixed layer of water existed across the core of the eddy. This resulted in the formation of a surface duct above the eddy duct. In the winter case, the eddy duct would reach all the way to the surface. Below the eddy duct, there is, of course, the deep ocean sound channel with an axis depth of 1000 meters. Since we are interested in frequencies down to 10 Hz, you might expect us to get below the cutoff frequencies for the two upper ducts. Hence, sound would begin to leak from these ducts into the deep sound channel. This frequency dependence is not handled by ray theory unfortunately.

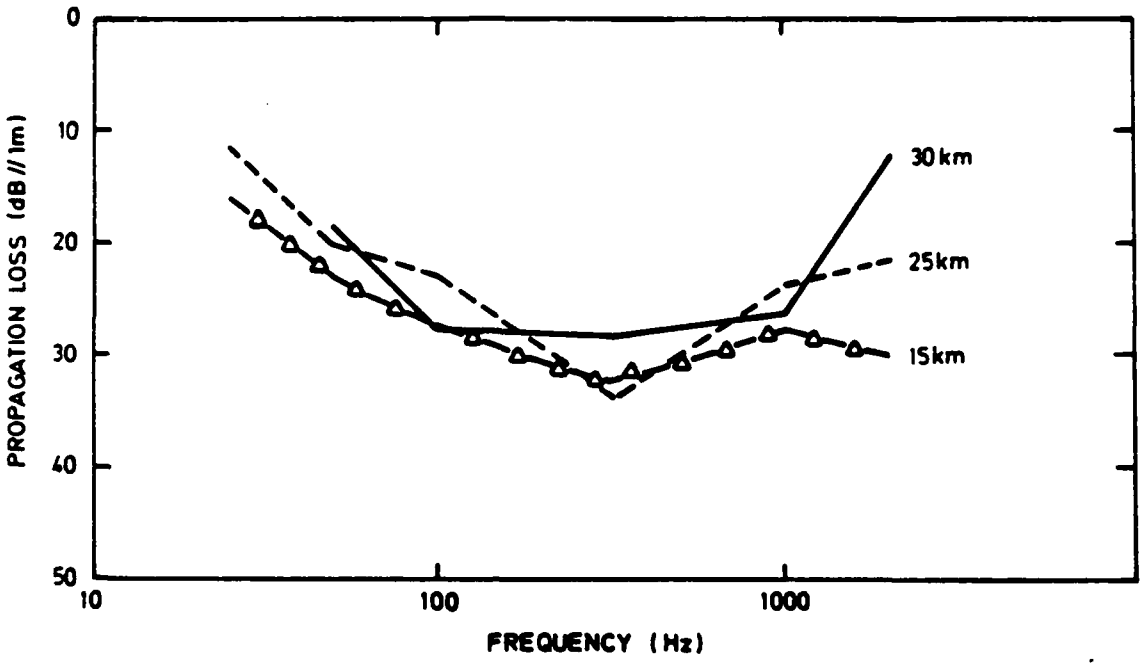

DIFFERENTIAL PROPAGATION LOSS BETWEEN SHALLOW AND DEEP CHARGES AT 15 25 AND 30 km.

Slide 8

The major propagation effects predicted by ray theory were verified by the experiment; moreover, the suspected frequency dependence did appear. Here we have the differential propagation loss, comparing propagation loss from sources in the eddy duct and sources in the surface duct to a receiver in the eddy duct. Results at various ranges are plotted against frequency. It shows that this difference is frequency dependent with a maximum occurring at about 300 Hz.

We could speculate as to the cause, but were stymied by the lack of a frequency-dependent sound propagation prediction model that was also range-dependent.

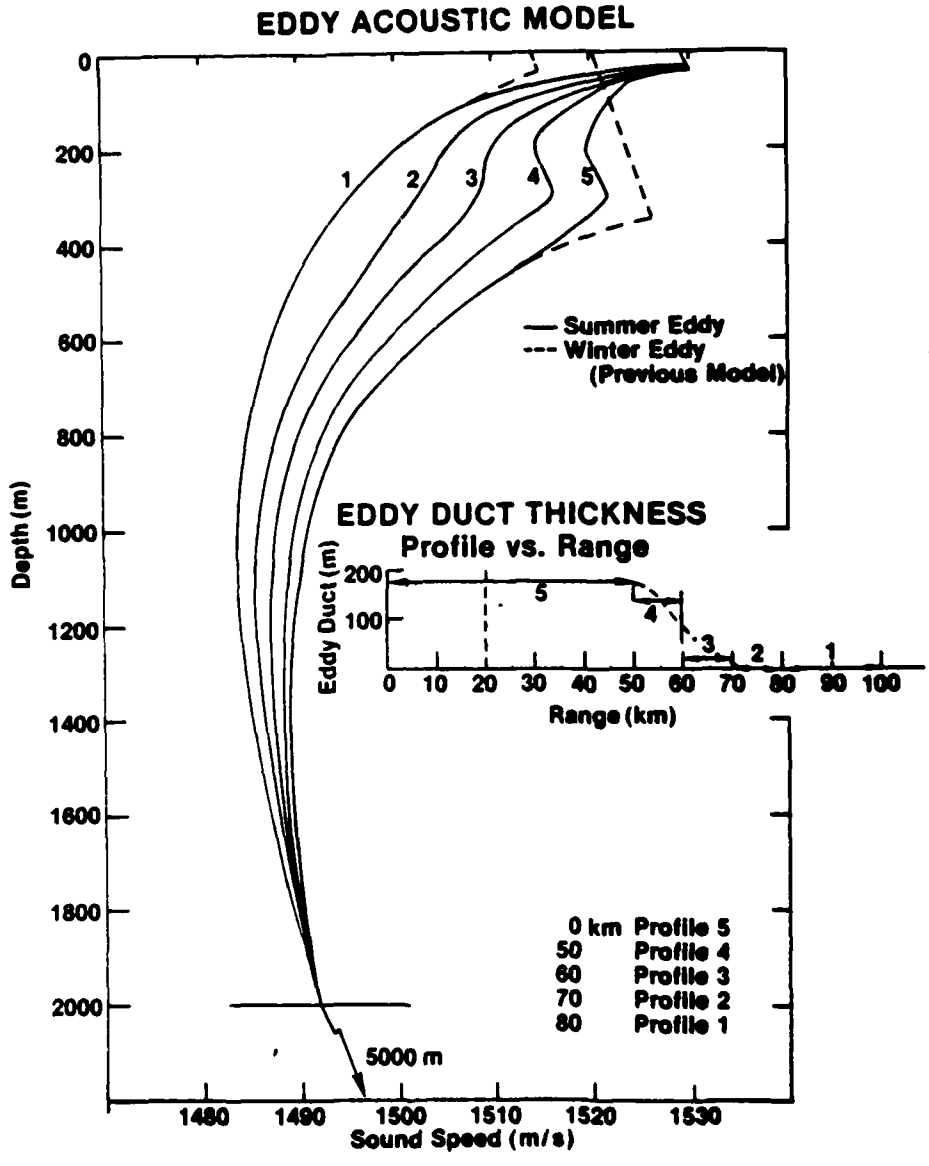

Slide 9

A breakthrough for us came with the introduction (just in time to get results for this paper) of a finite difference version of the parabolic equation prediction model by Dr. Ding Lee of NUSC. The model is still under development so we are not looking too hard at absolute levels, but it does seem to give us for the first time an insight into the cause of the frequency dependence in the eddy propagation.

As with the earlier work, we used a series of profiles measured in an eddy — this time under summer conditions. The center profile (Range 0) being number 5. You can see that the principal difference between summer and winter conditions is the warm surface layer in the summer. A winter profile is shown by dashed line.

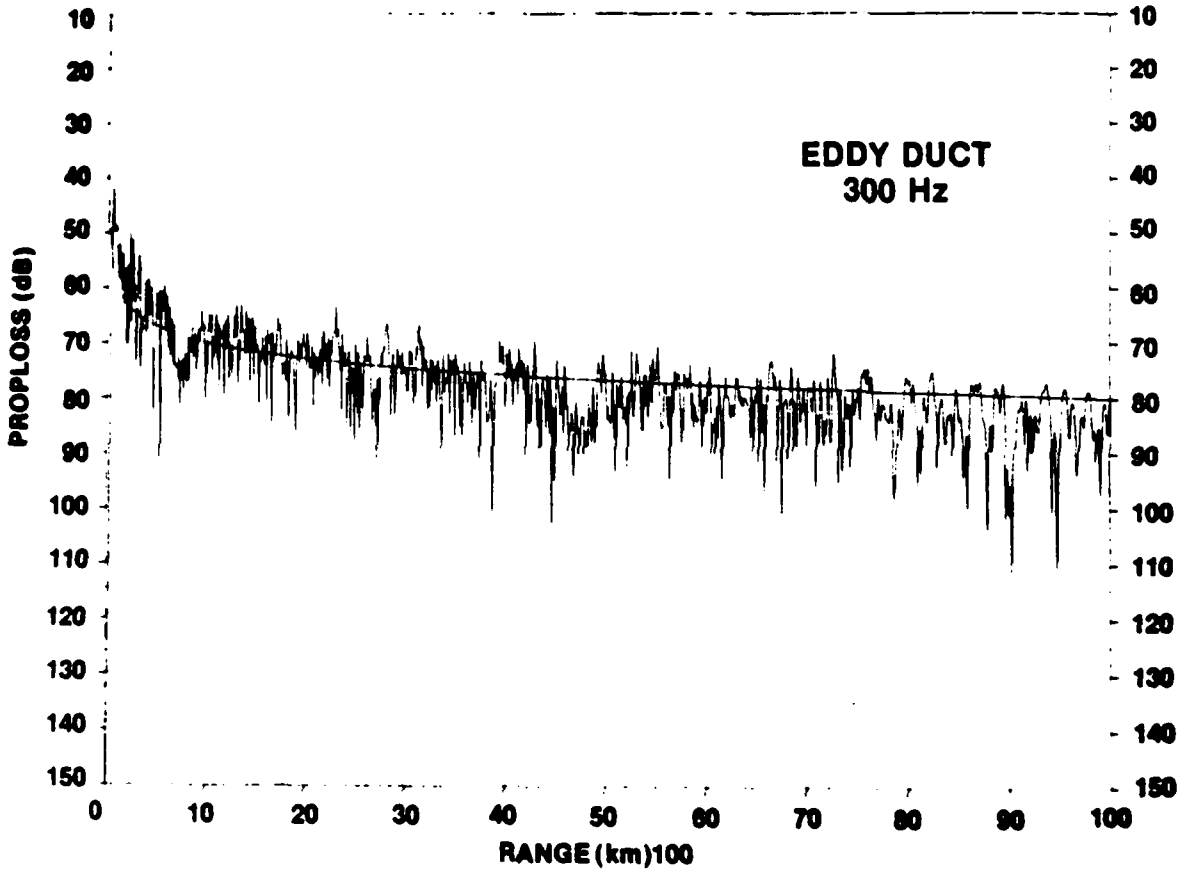

Slide 10

To illustrate the phenomenology in a limited time, we will just show the case of sound propagation with both source and receiver in the eddy duct.

At 300 Hz, the energy is entirely trapped in the duct so we have typical sound channel propagation. The solid line is normal spreading loss in a sound channel — the slight difference is due to attenuation.

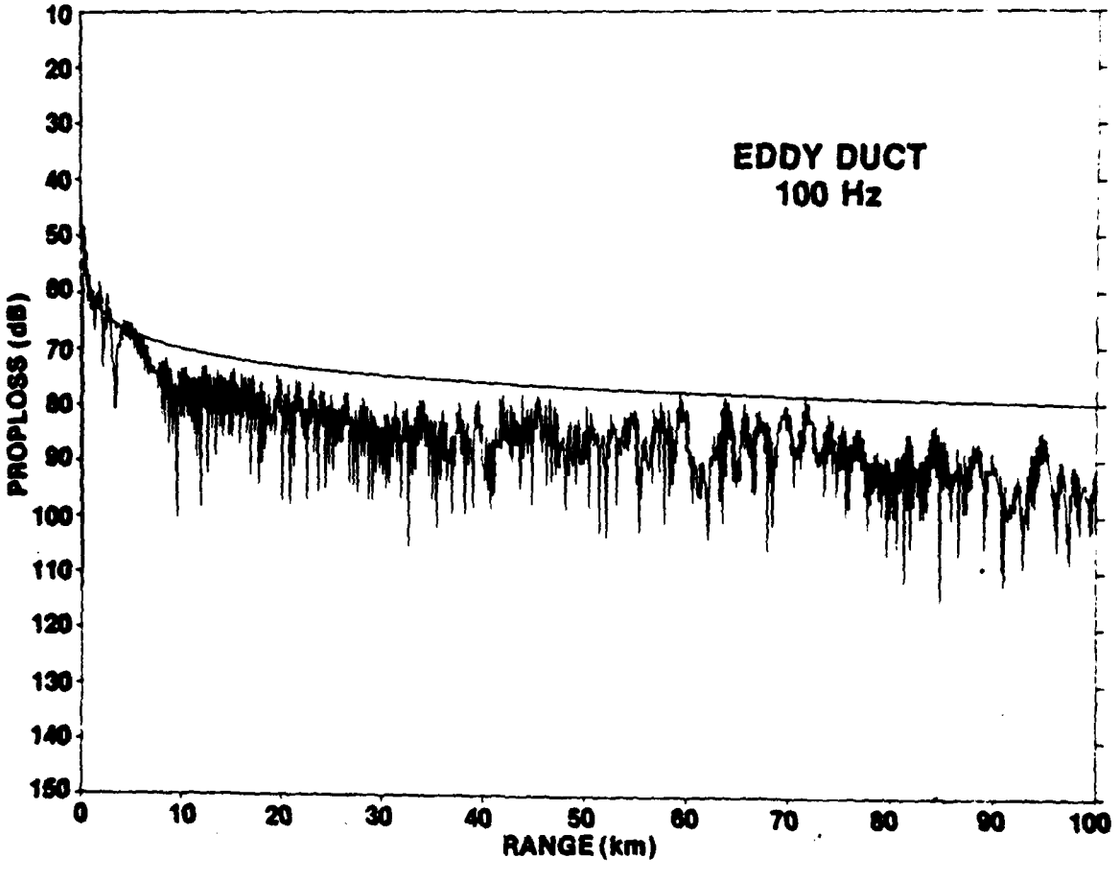

Slide 11

At 100 Hz, the level is somewhat reduced indicating that some energy is starting to leak out of the eddy duct into the deep sound channel. As you can see, the eddy duct mode of propagation still dominates.

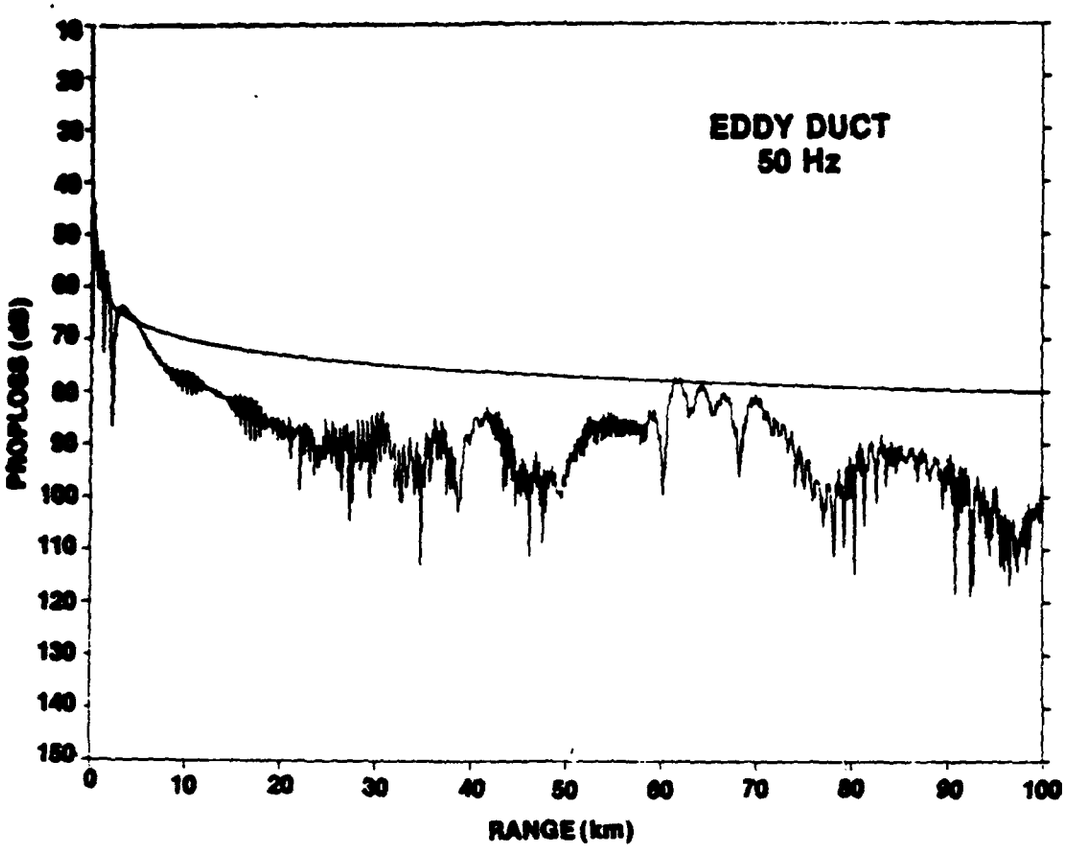

Slide 12

At 50 Hz, we see a distinct change in the pattern. Energy is leaking from the eddy duct at a relatively high rate as indicated by the initial drop in level. However, once this energy reaches the deep sound channel, it is refracted back as a convergence zone — the 50-80 kilometer range. So we now have two competing effects, the eddy duct propagation mode and the deep sound channel mode (the relative importance being determined by the frequency).

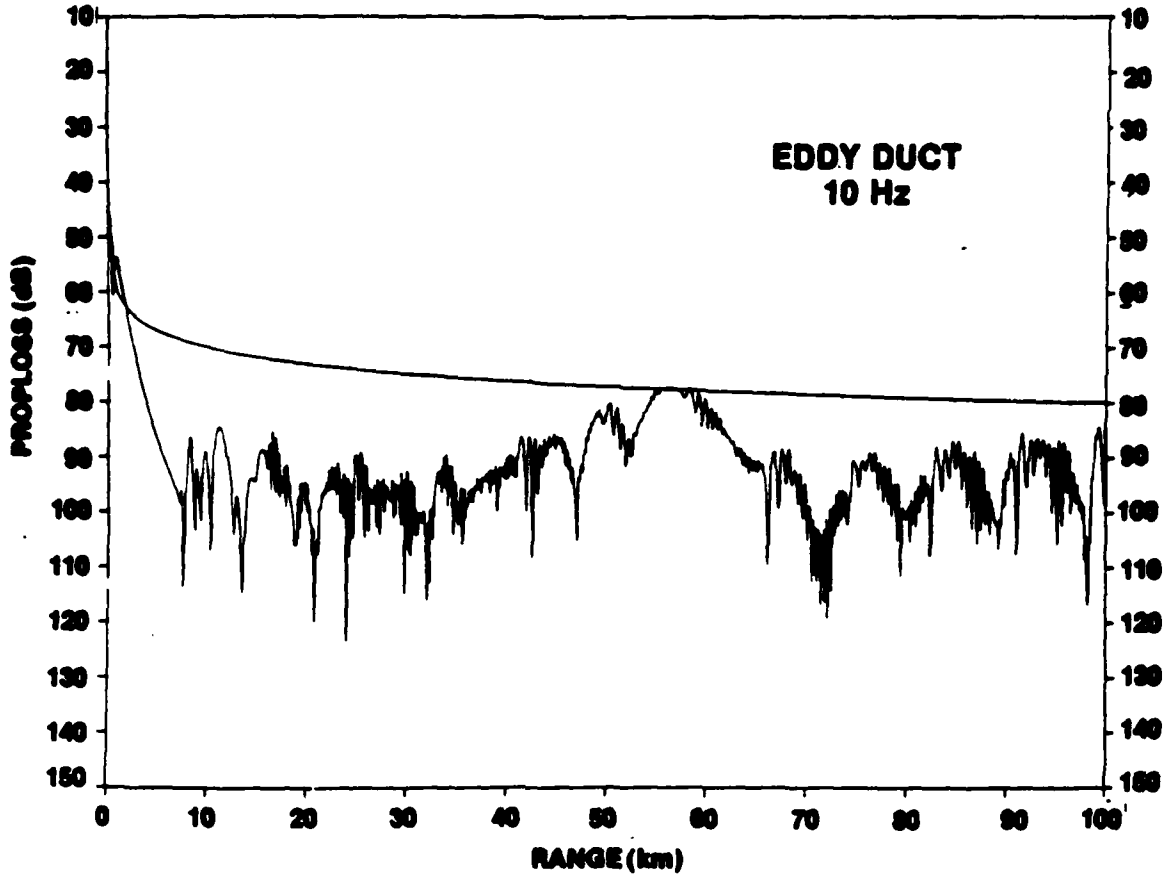

Slide 13

At 10 Hz, the relative importance of the deep sound channel mode is increased further. And as a result, propagation loss does not simply decrease with range.

The exact level will, of course, depend on the shape of the eddy duct and deep sound channel and the rate at which the eddy duct tapers down.

For the present, our calculations are limited by computer capacity to frequencies of 300 Hz or lower, but we are hoping to extend our capability to all frequencies of interest soon.

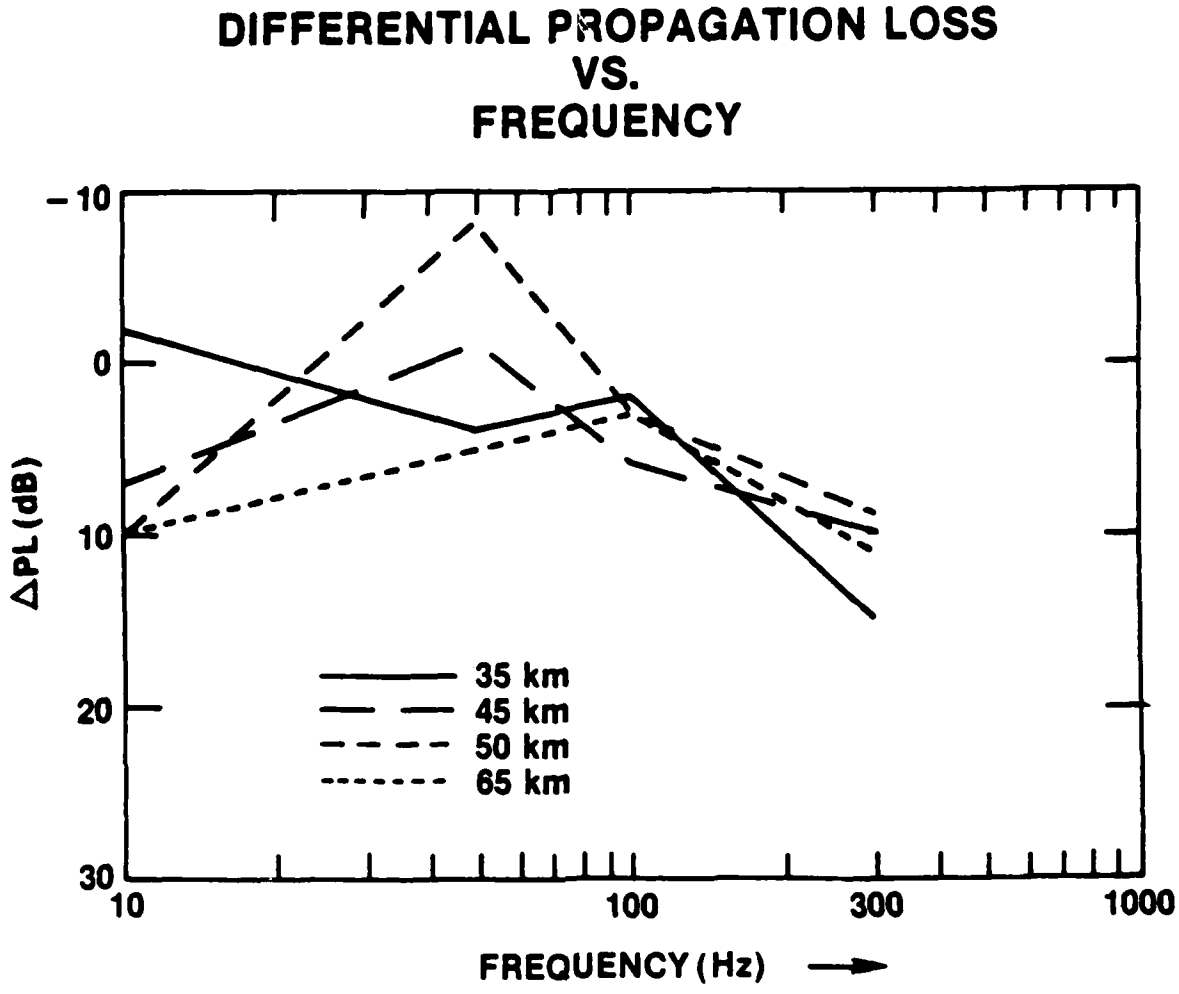

Slide 14

Our final result is the frequency-dependence predictions at various ranges. In general, it has the same trend as was measured experimentally. At very low frequencies, it predicts that the differential propagation loss will vary considerably with range due to the contribution of the convergence zone.

Summary

In summary, the major frequency-independent effects of eddies on sound propagation are now understood. We now have the modeling tools to quantify the frequency-dependent effects and the results to date look very promising.

Thank you.

Initial Distribution List

ADDRESSEE	NO. OF COPIES
NAVMAT (CAPT D. F. Parrish (MAT 08L), CAPT E. Young (MAT 0724))	2
NRL (B. Adams, R. Heitmeyer, A. Berman, Dr. K. M. Guthrie (Code 5160))	4
NOSC, San Diego (J. R. Lovett, Dr. R. Buntzen, Library)	3
NADC, Warminster	1
NCSL, Panama City	1
NPS, Monterey (Prof. C. N. Mooers, Prof. H. Medwin, Library)	3
NORDA, NSTL Station (R. Martin, R. Lauer, R. R. Goodman)	3
ONR (G. R. Hamilton, L. E. Hargrove (Code 421))	2
ONRWEST (CDR R. Lawson, B. J. Cagle)	2
COMTHIRDFLT (CDR J. Carlmark)	1
DARPA (CAPT V. P. Simmons)	1
NAVSEASYSCOM (C. D. Smith (Code 63R), R. W. Farwell (Code 63RA))	2
NUSC, Tudor Hill	1
COMNAVMARIANAS (CDR R. R. Miller)	1
University of Auckland (Prof. A. C. Kibblewhite)	1
Materials Research Laboratories (Dr. Daniel J. Whelan)	1
Deputy Cons. for Defence Science, Embassy of Australia (Dr. D. Wyllie)	1
Defence Scientific Establishment (Dr. Bert Olsson)	1
FWG (Dr. H.-G. Schneider)	1
Brown University, Dept. of Physics (Dr. Robert Beyer)	1
Catholic University of America, Dept. of Mechanical Engineering (Dr. Robert J. Urick)	1
University of Houston, Cullen College of Engineering (Dr. Bill D. Cook)	1
Royal Australian Navy Research Laboratory (Dr. Martin Lawrence, Dr. Carl Nilsson)	2
Admiraltiy of Underwater Weapons Establishment (Dr. David E. Weston)	1
Instituto de Pesquisas da Marinha (CDR Carlos Parente)	1
Yale University, Dept. of Engineering and Applied Science (Dr. John G. Zornig)	1
University of Tennessee, Dept. of Physics (Dr. Mack A. Breazeale)	1
Georgetown University, Physics Department (Dr. Walter G. Mayer)	1
Case Western Reserve University (Dr. Ernest B. Yeager)	1
Scripps Institute (Dr. F. H. Fisher, Dr. W. H. Munk Dr. R. E. Stevenson)	3
University of Rhode Island, Dept. of Physics (Dr. Stephan Letcher)	1
APL/University of Texas (Dr. L. Hampton)	1
University of Bath, School of Physics (Dr. H. O. Berktay)	1
Defence Research Establishment, Atlantic (Dr. H. M. Merklinger)	1
Defence Research Establishment, Pacific (Dr. Robert Chapman)	1
University Louis Pasteur (Prof. S. Candau)	1
Technical University of Denmark (Dr. Leif Bjorno)	1
Defence Research Centre, Salisbury (Dr. Dennis H. Brown)	1
Laboratorie De Acoustica Submarina (Dr. Jorge Novarini)	1
DTIC	12